
emc2
ENERGY MATERIALS CENTER AT CORNELL

# Road map

- Introduction
  - Brief introduction to fuel cells and batteries
  - Why X-rays?
- Representative studies
  - Fuel cells
    - In-situ studies of PtBi; XRD, XAS
  - Batteries
    - MnOx For Lithium Anode
    - XRD of Organics
    - In-Situ XAS and XRD of Sulfur
- Conclusions and future directions

# Why Fuel Cells?

In principle, a fuel cell can convert chemical energy to electrical (and thus mechanical) energy **more efficiently** than internal combustion (heat) engines or even turbines due to Carnot Cycle limitations of heat engines.

## Carnot Cycle

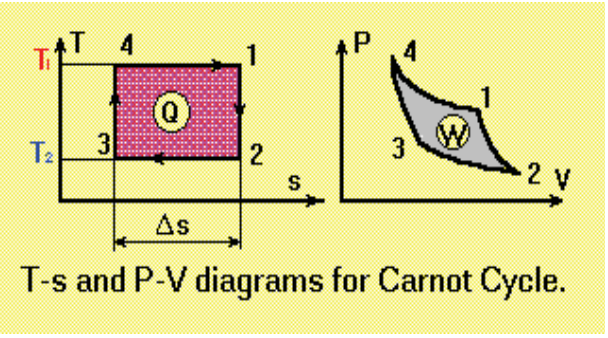


T-s and P-V diagrams for Carnot Cycle.

## Heat Engine

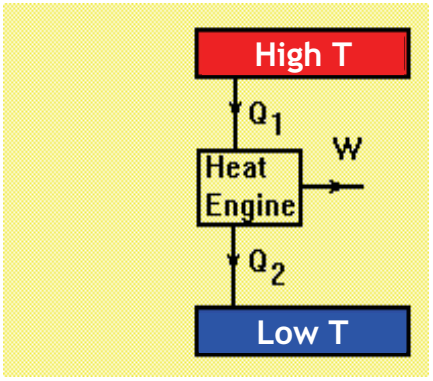


$Q_1 > W$, $Q_2 > 0$

Thermal efficiency $\eta = T_h - T_c / T_h$

# U.S. Energy Production and Usage in 2008

*Units in Quadrillion BTUs (Quads)*

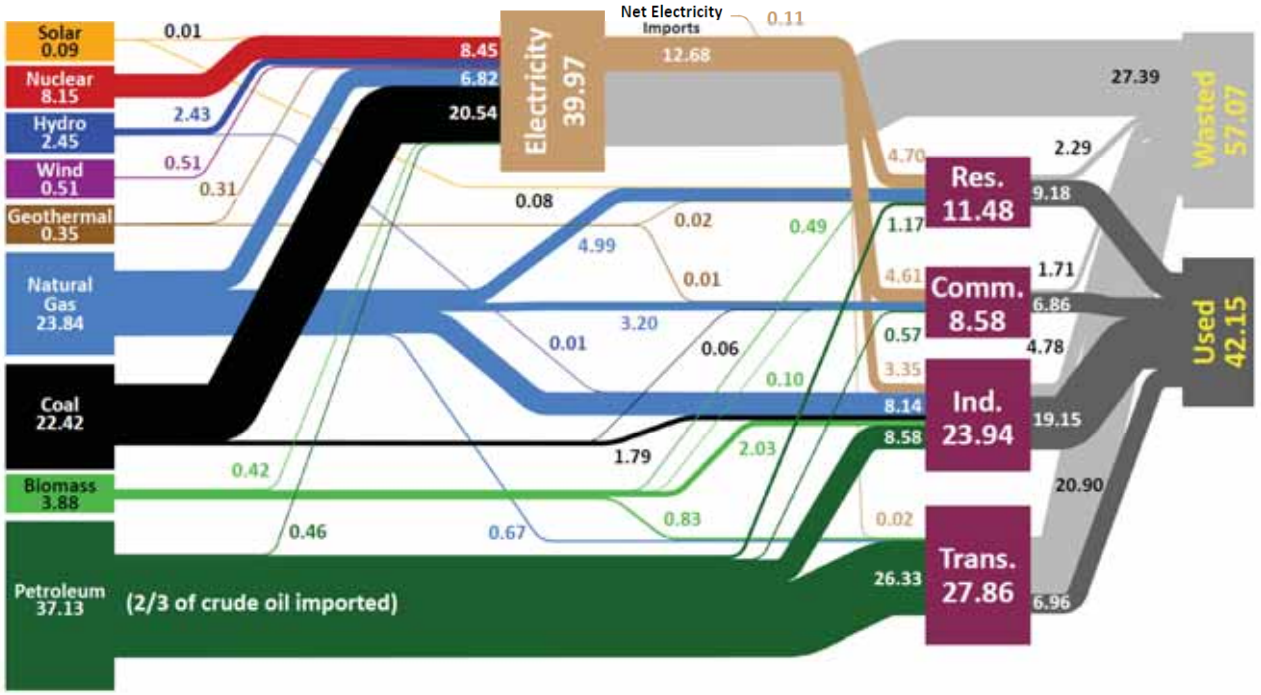


*Source: Lawrence Livermore National Laboratory and the Department of Energy, Energy Information Administration, 2009 (based on data from DOE/EIA-0384(2008), June 2009).*

U.S. DEPARTMENT OF ENERGY | Office of Science



Courtesy: H. Kung @ DOE

# Electrical Energy Storage Is A Key Need for the Nation's Future

***Achieving an electric fleet and storing energy from intermittent sources will not be possible without innovations in electrical energy storage***

- These applications place great demands on energy storage
  - Higher energy and power densities
  - Appropriate recharge rates
  - Long life cycle
  - Reliability
  - Safety

US in 1900
1500 electric cars compared with
1000 ICE cars

# X-rays, batteries & fuel cells

Practical Battery

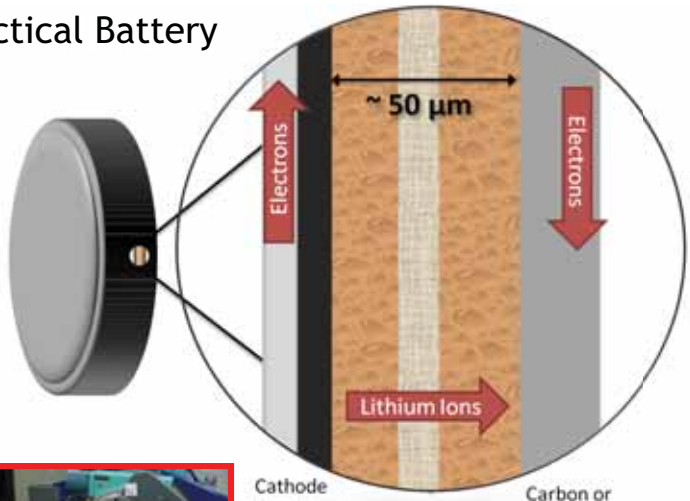


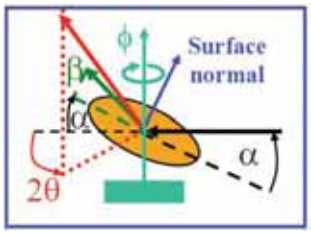


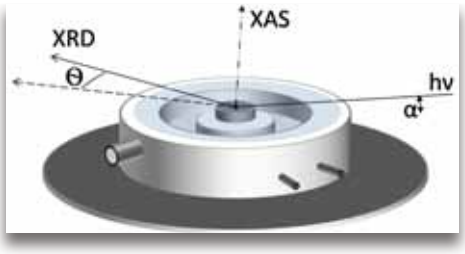


- X-rays make it possible . . .
  - Buried Interfaces/Volumes
  - Ex-Situ, In-Situ, Operational
  - Phase and Element-specific
- In-situ studies of fuel cell electrocatalysts & battery materials
- Changes in electrocatlyst's structure & composition
  - Batteries
    - Half of cell can use lithium
      - Probing reactions of volumes, not just interfaces
      - Time scale is tied to solid-state reactions

# PtBi Ordered Intermetallic In-situ Grazing Incidence Diffraction

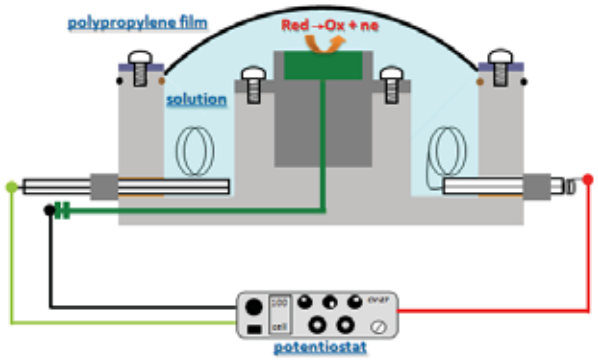


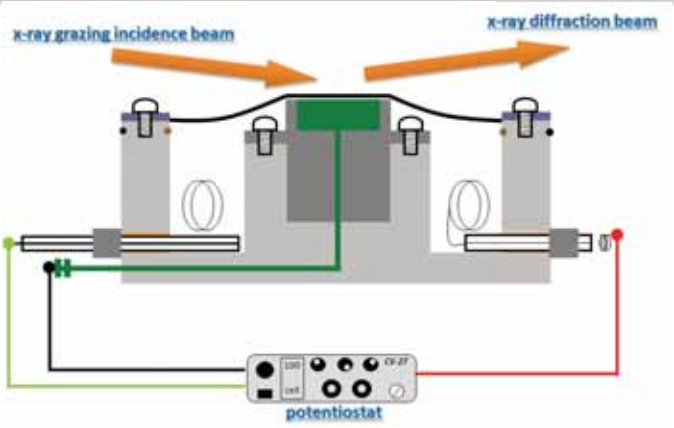


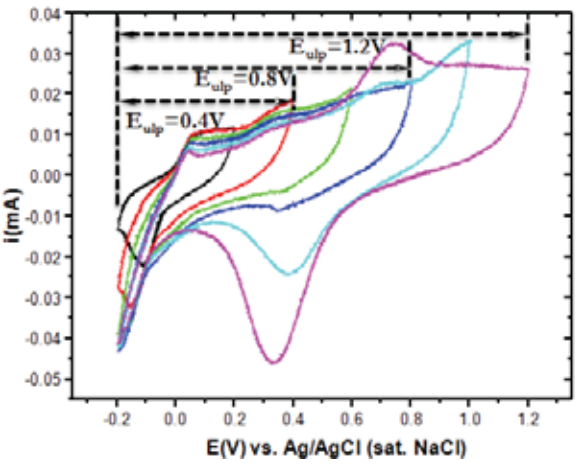


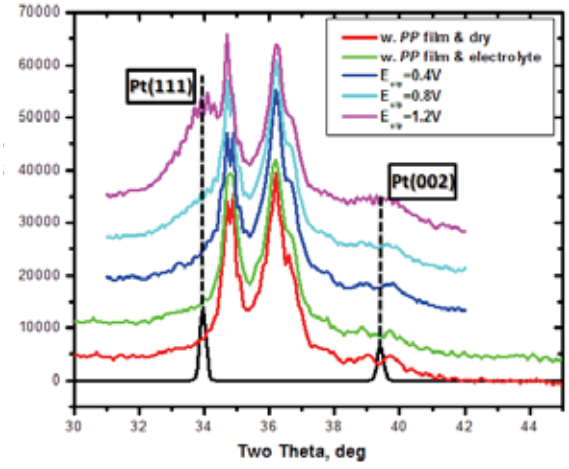


Pt crystalline structure ~5nm

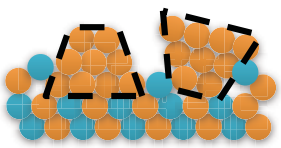

external Pt island physical size ~200nm

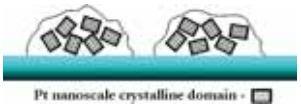

# XAS & EXAFS

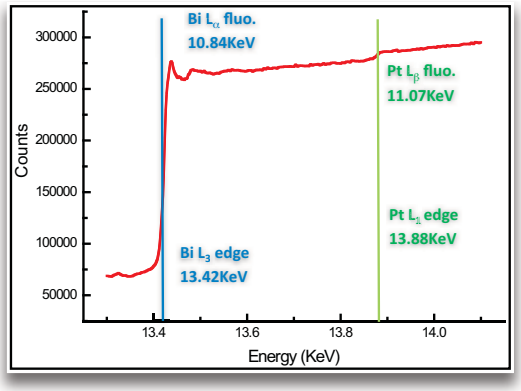
Bi Lα fluo.
10.84KeV
Pt Lβ fluo.
11.07KeV
Pt LII edge
13.88KeV
Bi L3 edge
13.42KeV
Counts
Energy (KeV)

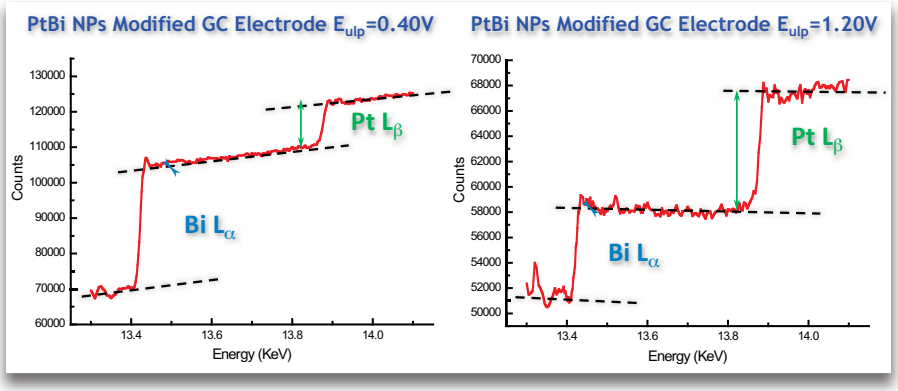
PtBi NPs Modified GC Electrode Eulp=0.40V
PtBi NPs Modified GC Electrode Eulp=1.20V
Pt Lβ
Bi Lα
Counts
Energy (KeV)

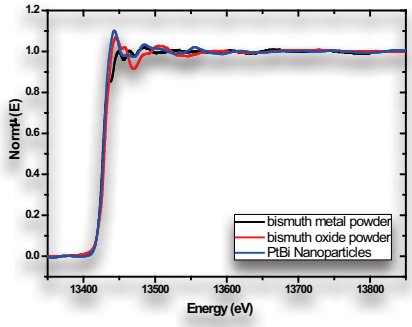
Norm(E)
Energy (eV)
bismuth metal powder
bismuth oxide powder
PtBi Nanoparticles

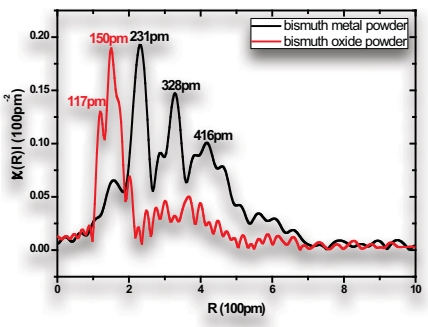
150pm
231pm
117pm
328pm
416pm
bismuth metal powder
bismuth oxide powder
|K(R)| (100pm)-2
R (100pm)

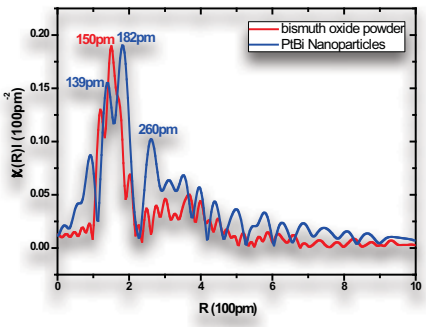
150pm
182pm
139pm
260pm
bismuth oxide powder
PtBi Nanoparticles
|K(R)| (100pm)-2
R (100pm)

# Battery Cell for *In-Situ* X-ray Studies


## *Systems Studied:*

- Manganese Oxide Anodes (XAS, XRD)
- Organosulfur Cathodes (XRD)
- Elemental Sulfur Cathodes (XAS, XRD)

**Diffraction/XAS**
Transmission

**XAS**
Fluorescence Mode

# Next-Generation Lithium Battery Anodes

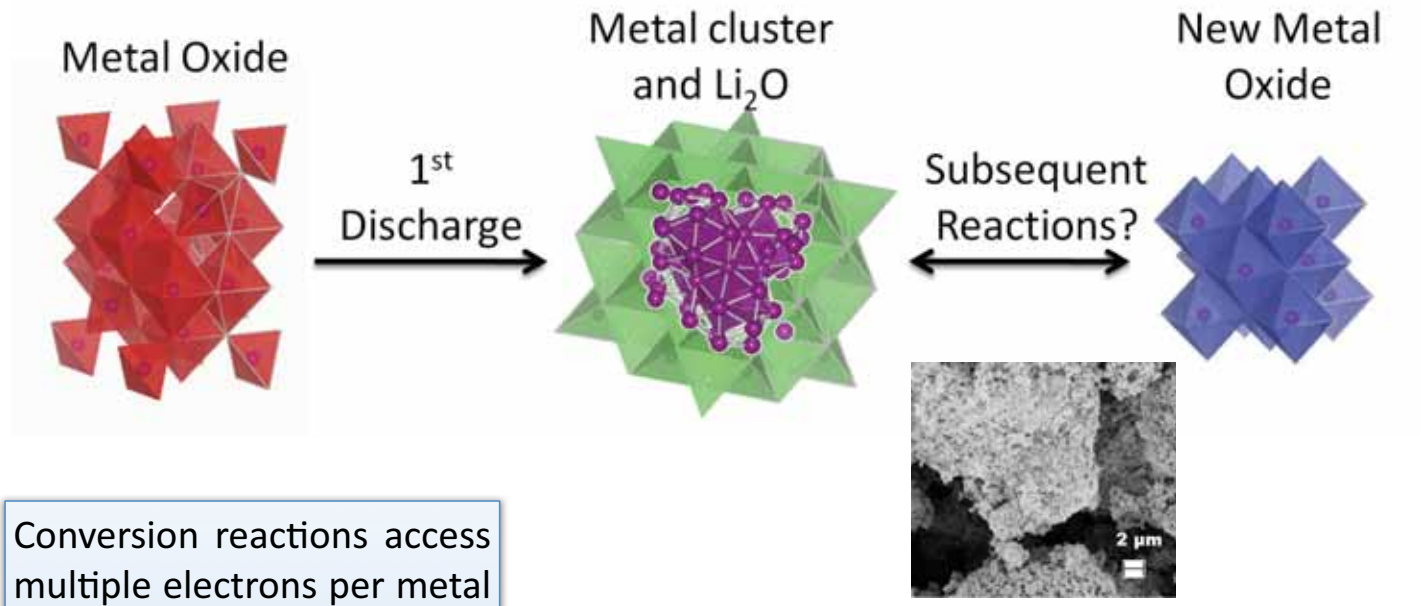





Conversion reactions access multiple electrons per metal atom

With "appropriate" particle size and composition, near-theoretical capacity is attained for >10s of cycles

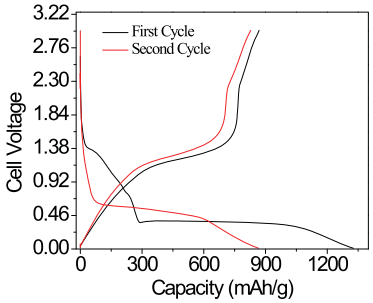


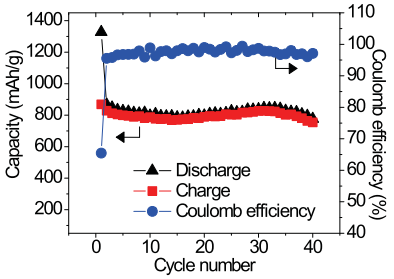

# Summary of Mechanism

**Amorphous MnOx ($Mn_5O_8$)**

I A

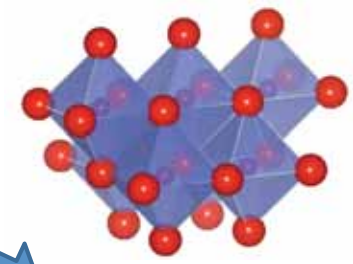

**MnO**
Crystalline domain radius 0.5 to 1 nm

II

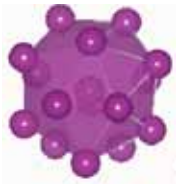

**Mn**
Ordered radius 0.5 to 1 nm

III

**Solid Electrolyte Interface Formation**

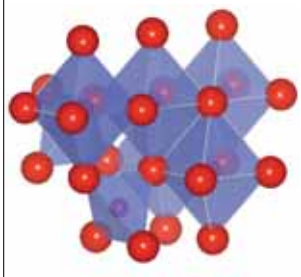

I B

**Rapid reaction of each domain**

**Nucleation and growth of Mn clusters**

**Reversible Capacity in "Solid Solution" of MnO/Mn**

IV

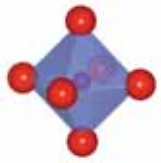

**$Mn_3O_4$**
Crystalline domain radius ~15 nm

**MnO**
Disordered beyond 1 bond length

# Why Lithium-Sulfur Batteries?

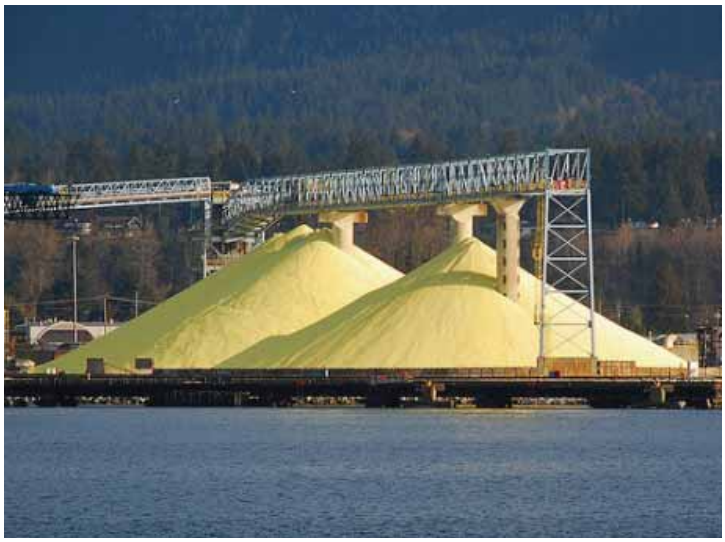

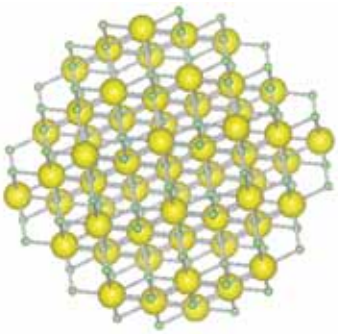

$$8Li_2S \rightleftharpoons S_8 + 16Li^+ + 16\ e^-$$

1.67 Ah/g
2.6-4.2 Wh/g
~ $0.02/g

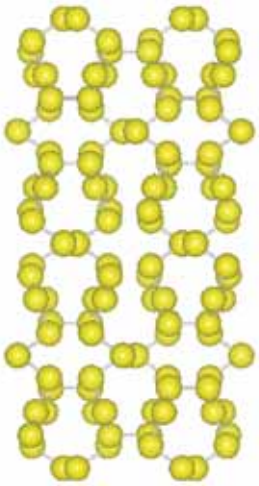

# Redox Behavior of $S_8$ in N, N′-Dimethylformamide

*J. Electroanal. Chem.* **440** 243 (1997)
*J. Electroanal. Chem.* **432** 129 (1997)
*J. Electroanal. Chem.* **420** 167 (1997)
*J. Electroanal. Chem.* **398** 77 (1995)

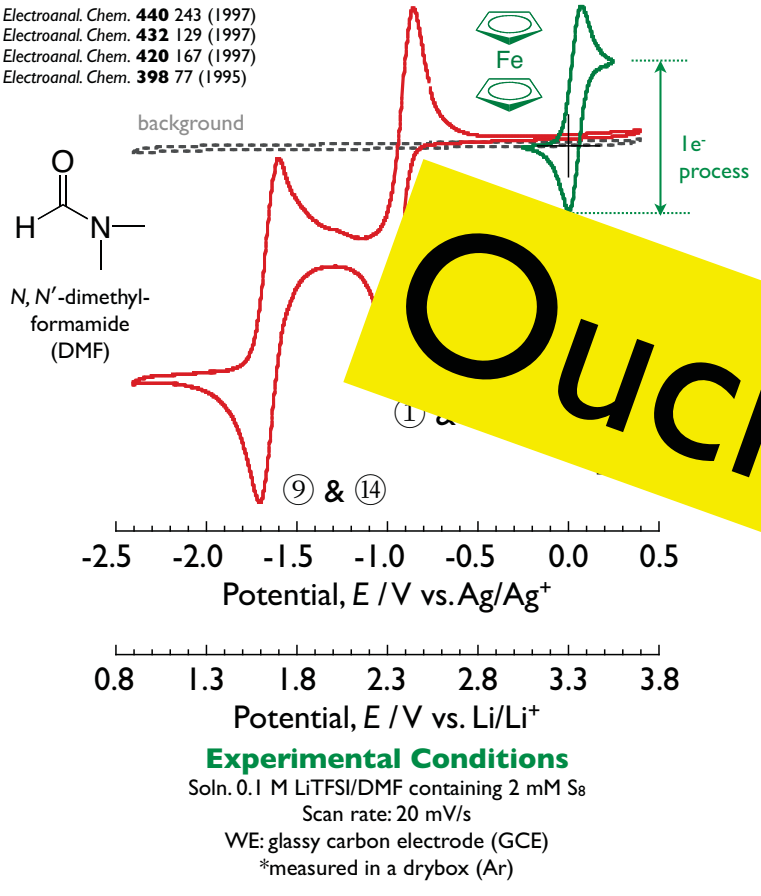





*N, N′*-dimethyl-formamide (DMF)

**Experimental Conditions**
Soln. 0.1 M LiTFSI/DMF containing 2 mM $S_8$
Scan rate: 20 mV/s
WE: glassy carbon electrode (GCE)
*measured in a drybox (Ar)

Ouch!!!

① $S_{8c} + e^- = S_{8c}^{\bullet -}$ (E step)
② $S_{8c}^{\bullet -} = S_{8l}^{\bullet -}$
③ $S_{8l}^{\bullet -} + e^- = S_{8l}^{2-}$ (E step)
④ $S_{8c}^{\bullet -} + S_{8l}^{\bullet -} = S_{8c} + S_{8l}^{2-}$
⑤ $S_{8l}^{2-} = S_6^{2-} + 1/4 S_{8c}$
⑥ $S_{8c}^{\bullet -} + S_6^{2-} = S_{8c}^{2-} + S_6^{\bullet -}$
[illegible] $+ S_6^{2-} = S_{8l}^{2-} + S_6^{\bullet -}$
[illegible] E step)
[illegible] $S_4^{2-}$ (disproportionation)
[illegible] $S_{8l}^{2-}$ (disproportionation)
⑫ $S_4^{2-}$
⑬ $S_{8l}^{2-} = 2S_4^{\bullet -}$
⑭ $S_4^{\bullet -} + e^- = S_4^{2-}$ (E step)
⑮ $S_3^{\bullet -} + S_4^{2-} = S_3^{2-} + S_4^{\bullet -}$

soluble species in solution

insoluble species precipitated

⑯ $S_2^{\bullet -} + e^- = S_2^{2-}$ (E step)
⑰ $S_2^{2-} = 2S_1^{\bullet -}$
⑱ $S_1^{\bullet -} + e^- = S_1^{2-}$ (E step)

# Possible Mechanisms

| Researcher | Proposed Mechanism | X-Ray Observables |
|---|---|---|
| Kolosnitsyn | Unimolecular Decomposition<br>$S_8^{2-} + 2\,e^- \rightleftharpoons S_7^{2-} + Li_2S$ | $Li_2S$ appears throughout discharge |
| Na | Progressive reduction of solution-phase<br>$Li_2S_{2,sol} + 2\,e^- \rightleftharpoons Li_2S_{sol}$ | the end of<br>S signal from |
| White | Progressive reduction of polysulfides in solution; reduction of lowest polysulfides ($S_2^{2-}$, $S^{2-}$) during 2nd plateau | $Li_2S$ appears throughout 2nd plateau |

**No in-situ measurements of $Li_2S$!**
**No in-situ speciation of reaction intermediates!**

# Sulfur Disappearance 2D Diffraction Movie

- Sulfur crystal structure disappears during reduction
- Dynamic process for large crystals – reflections may decrease, increase, or stay the same between images

# Conclusions & Outlook

The use of x-rays is enabling in-situ studies of energy materials and interfaces providing extraordinary levels of structural, compositional and mechanistic details.

Sources like the ERL (and new detectors) will enable diffraction/spectroscopy experiments with truly unprecedented levels of spatio-temporal resolution; down to the single particle, in-situ and in real time.

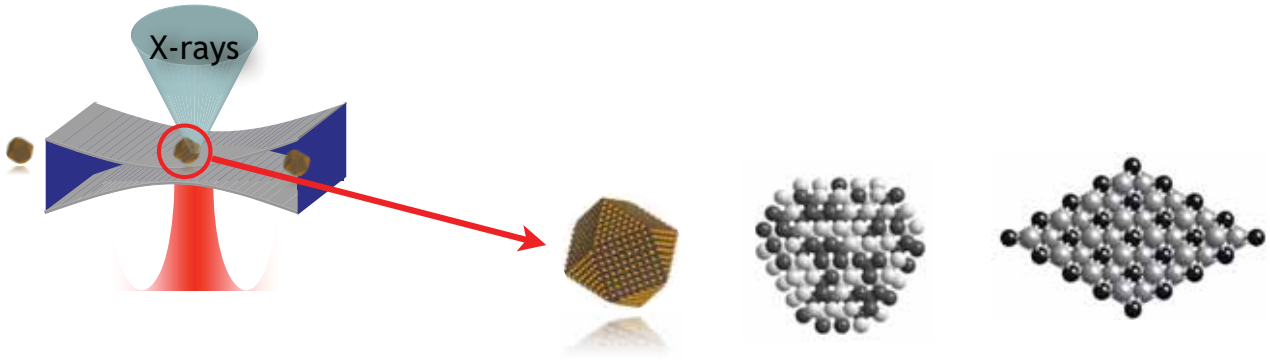

# New X-ray Detector

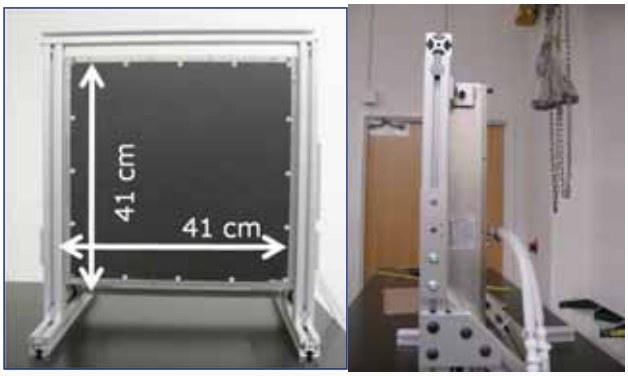


- Adapt mammography detector developed by GE
- 41x41cm
- 200x200µm pixels
- readout rates up to 30 Hz

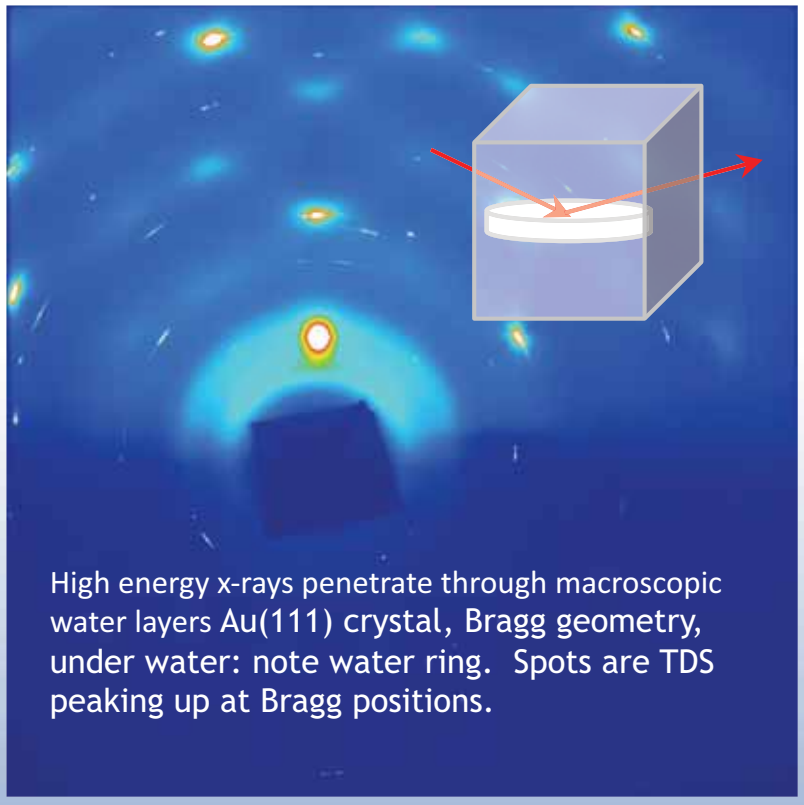

High energy x-rays penetrate through macroscopic water layers Au(111) crystal, Bragg geometry, under water: note water ring. Spots are TDS peaking up at Bragg positions.

# Abruña Group Battery Researchers

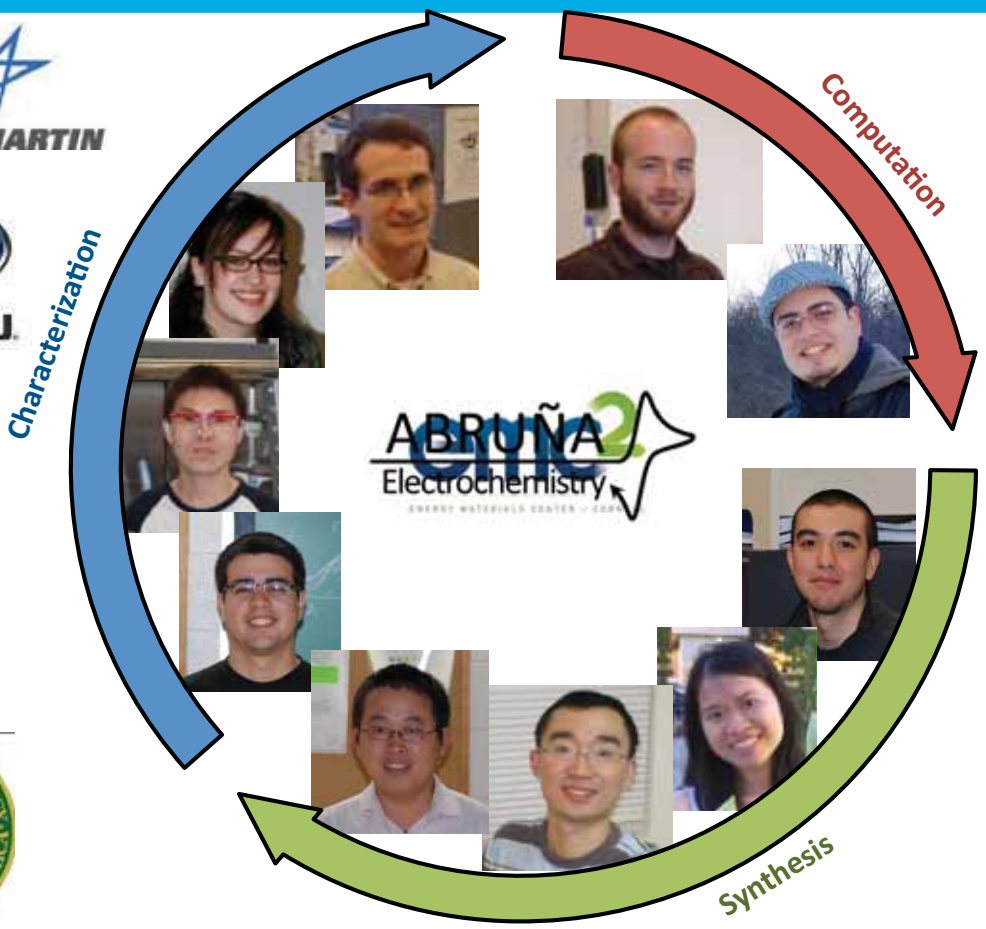


**Yi Liu, Detlef Smilgies, Ken Finkelstein, Darren Dale, Alex Kazimirov**
**Prof. Joel D. Brock**


NSF
Office of Basic Energy Sciences
Serving the Present, Shaping the Future
DEPARTMENT OF ENERGY
UNITED STATES OF AMERICA
emc2
ENERGY MATERIALS CENTER at CORNELL
CORNELL CENTER FOR MATERIALS RESEARCH
cfci
SUBARU
Sumitomo Corporation
LOCKHEED MARTIN
CORNELL
CNF
Cornell Nanofabrication Facility
NSF
FUTURE ENERGY SYSTEMS
GM
MOTOROLA
NYSTAR
CAT
CENTER FOR NANOSCALE SYSTEMS
Ford

# *Powered by:*


As featured in the Oct. 2001 issue of National Geographic.


Culebra, Puerto Rico


"That's
all
folks!"